Organic &
Biomolecular
Chemistry

Accepted Manuscript

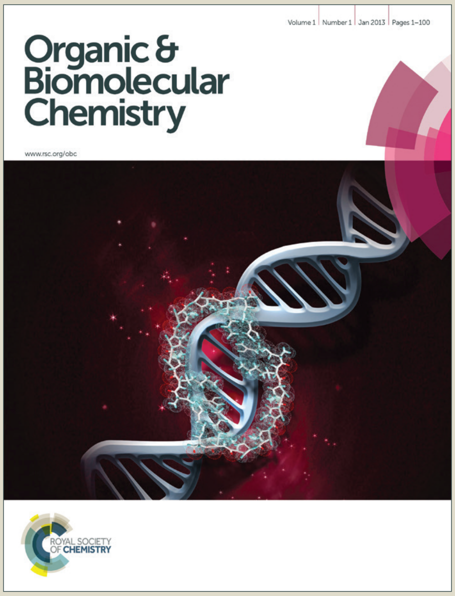

ROYAL SOCIETY
OF CHEMISTRY

www.rsc.org/obc

Organic & Biomolecular Chemistry RSCPublishing

REVIEW

Organic synthetic transformations using organic dyes as photoredox catalysts

Cite this: DOI: 10.1039/x0xx00000x

Received 00th January 2012,
Accepted 00th January 2012

DOI: 10.1039/x0xx00000x

www.rsc.org/

Shunichi Fukuzumi and Kei Ohkubo

The oxidizing ability of organic dyes is enhanced significantly by the photoexcitation. Radical cations of weak electron donors can be produced by electron transfer from the donors to the excited states of organic dyes. Radical cations thus produced undergo bond formation reactions with various nucleophiles. For example, the direct oxygenation of benzene to phenol was made possible under visible-light irradiation of 2,3-dichloro-5,6-dicyano-*p*-benzoquinone (DDQ) in an oxygen-saturated acetonitrile solution of benzene and water via electron transfer from benzene to the triplet excited state of DDQ. 3-Cyano-1-methylquinolinium ion ($QuCN^+$) can also act as an efficient photocatalyst for selective oxygenation of benzene to phenol using oxygen and water under homogeneous and ambient conditions. Alkoxybenzenes were also obtained when water was replaced by alcohol under otherwise the same experimental conditions. $QuCN^+$ can also be an effective photocatalyst for the fluorination of benzene with O_2 and fluoride anion. Photocatalytic selective oxygenation of aromatic compounds were achieved using an electron donor-acceptor linked dyad, 9-mesityl-10-methylacridinium ion (Acr^+–Mes) as a photocatalyst and O_2 as an oxidant under visible light irradiation. The electron-transfer state of Acr^+–Mes produced upon photoexcitation can oxidize and reduce substrates and dioxygen, respectively, leading to selective oxygenation and halogenation of substrates. Acr^+–Mes has been utilized as an efficient organic photoredox catalyst for many other synthetic transformations.

Introduction

The rapid consumption of fossil fuels causes not only the depletion but also unacceptable environmental problems such as green house effects, which would lead to disastrous climatic consequences.[1,2] Because fossil fuels are products of photosynthesis, development of artificial photosynthesis for production of sustainable and clean energy resources using solar energy has merited increasing attention in order to solve global energy and environmental issues.[2-10] Photosynthesis is initiated by photoinduced electron-transfer reactions in the photosynthetic reaction centres. Thus, photoinduced electron-transfer pathways play a pivotal role to maintain the life on the planet. A variety of photosynthetic reaction centre models composed of electron donors and acceptors linked by covalent

*Department of Material and Life Science, Graduate School of Engineering, Osaka University, ALCA, Japan Science and Technology Agency (JST), Suita, Osaka
565-0871, Japan. E-mail: fukuzumi@chem.eng.osaka-u.ac.jp;
Fax: +81 6 6879 7370; Tel: +81 6 6879 7368*

Shunichi Fukuzumi

Shunichi Fukuzumi earned Ph.D. degree in applied chemistry at Tokyo Institute of Technology in 1978. He has been a Full Professor of Osaka University since 1994. He is now a Distinguished Professor of Osaka University and the director of an ALCA (Advanced Low Carbon Technology Research and Development) project.

Kei Ohkubo

Kei Ohkubo earned his Ph.D. degree in applied chemistry from Osaka University in 2001. He was working as a JSPS fellow and JST research fellow at Osaka University from 2001 to 2005. He has been a designated associate professor at Osaka University since 2005.

or non-covalent bonding have so far been developed, undergoing efficient charge separation and slow charge recombination.[11-22] Such photoinduced electron-transfer pathways enable to produce highly reactive radical cations and anions, leading to the discovery and design of novel organic synthetic transformations.[23-25]

Inorganic solid photocatalysts such as TiO_2 and ZnO have so far been frequently utilized as photoredox catalysts.[26-30] However, poor absorption of visible light by such inorganic photocatalysts has often limited their utilization for organic synthetic transformations using solar energies although some modified inorganic photocatalysts can absorb visible light.[26-30] In addition, selective photocatalytic oxygenation reactions with dioxygen has been difficult by using inorganic photocatalysts, because substrates were normally overoxidized up to CO_2 due to the extremely high oxidizing ability of the photoexcited state. In contrast to inorganic photocatalysts, organic photocatalysts can absorb visible light and the photoredox properties can be finely tuned by the rational design and synthesis.[31-33] Metal complexes with organic ligands have also been utilized as homogeneous photoredox catalysts for organic synthesis.[34-38] As compared with inorganic heterogeneous and homogeneous photocatalysts, organic photocatalysts have advantage with regard to lower cost, more synthetic versatility and more fine tuning of the redox properties. Thus, this review focuses on recent development of various organic synthetic transformations mediated by metal free organic photoredox catalysis under mild conditions.

Selective photocatalytic oxidation of benzene to phenol

Phenol is currently produced from benzene by a three-step cumene process, which is one of the most important chemicals in industry.[39] The cumene process affords very low yields (around 5%) with byproducts such as acetone and a methylstyrene.[39,40] Thus, extensive efforts have been devoted to achieve direct synthesis of phenol from benzene and oxygen, which is one of the dream chemical reactions, using heterogeneous inorganic catalysts.[40-47] However, the synthetic utility with inorganic catalysts has been limited because of low yield, poor selectivity, and the requirement of high temperature. In contrast to inorganic catalysts, selective oxidation of benzene to phenol was made possible under visible light irradiation of 2,3-dichloro-5,6-dicyano-*p*-benzoquinone (DDQ) in an oxygen-saturated acetonitrile (MeCN) solution of benzene and water (vide infra).[48]

The photooxidation of benzene occurs with DDQ and water to yield phenol and 2,3-dichloro-5,6-dicyanohydroquinone ($DDQH_2$) selectively.[48] The maximum quantum yield was 45%, indicating that the photochemical oxidation of benzene by DDQ is quite efficient.[48] DDH_2 can be oxidized with *tert*-butyl nitrite (TBN)[49] to regenerate DDQ under the aerobic conditions.[48] The catalytic oxygenation occurred to yield phenol (93%) with 98% conversion of benzene (30 mM) with DDQ (9.0 mM), TBN (1.5 mM) and water (0.5 M) after photoirradiation for 30 h.[48]

The catalytic mechanism is shown in Scheme 1. The photooxygenation of benzene to phenol is initiated by efficient intermolecular photoinduced electron transfer from benzene to the triplet excited state of DDQ ($^3DDQ^*$), because the free energy change for electron transfer determined from the one-electron oxidation potential of benzene (E_{ox} = 2.48 V *versus* SCE)[50,51] and the one-electron reduction potential of $^3DDQ^*$ (E_{red} = 3.18 V *versus* SCE)[52] is largely negative ($\Delta G_{et} = -0.70$ eV) and thereby exergonic. Benzene radical cation produced by photoinduced electron transfer from benzene to the triplet excited state of DDQ ($^3DDQ^*$) is converted to benzene π-dimer radical cation (λ_{max} = 900 nm) with benzene,[53,54] as detected by laser flash photolysis measurements.[48] Benzene radical cation, which is in equilibrium with benzene π-dimer radical cation, reacts with water to yield the OH-adduct radical, whereas $DDQ^{\bullet-}$ reacts with the OH-adduct radical to yield phenol and $DDQH_2$.[48] $DDQH_2$ is oxidized by the reaction with *tert*-butyl nitrite and O_2 via NO_2 to regenerate DDQ.[48] No further oxidation of phenol occurred.[48] Such selective oxidation of benzene to phenol results from the much faster back electron transfer from $DDQ^{\bullet-}$ to phenol radical cation as compared with the back electron transfer from $DDQ^{\bullet-}$ to benzene radical cation. The driving force of back electron transfer from $DDQ^{\bullet-}$ to benzene radical cation (1.97 eV) is much larger than that from

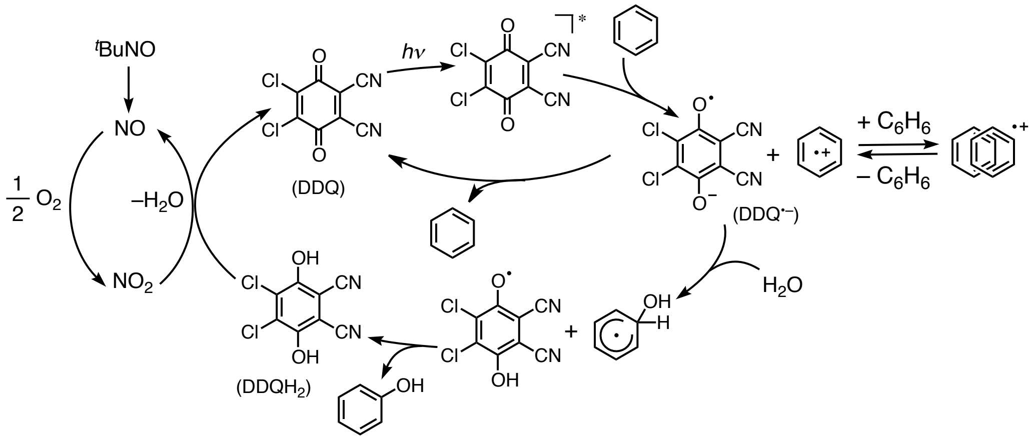

Scheme 1 Photocatalytic cycle of selective hydroxylation of benzene to phenol with O_2 and H_2O using DDQ and TBN as an organic photocatalyst and an oxidation catalyst of $DDQH_2$ with O_2, respectively.

$DDQ^{\bullet -}$ to phenol radical cation (1.09 eV).[48] In such a case, the back electron transfer from $DDQ^{\bullet -}$ to benzene radical cation occurs in the Marcus inverted region,[55] where the back electron transfer in the radial ion pair is much slower than the dissociation of radical ions.[48] In contrast, back electron transfer from $DDQ^{\bullet -}$ to phenol radical cation occurs at the Marcus top region, where the back electron transfer is much faster than the dissociation of radical ions.[48] This is the reason why the selective photocatalytic oxidation of benzene to phenol occurs without further oxidation of phenol.

3-Cyano-1-methylquinolinium perchlorate salt ($QuCN^+$ ClO_4^-) also acts as an efficient organic photocatalyst for selective hydroxylation of benzene to phenol under homogeneous and ambient conditions, where molecular oxygen and water are oxidant and oxygen source, respectively (Scheme 2).[56] In this case as well, benzene radical cation formed by photoinduced electron-transfer oxidation of benzene with the singlet excited state of $QuCN^+$ reacts with H_2O to yield the OH-adduct radical. On the other hand, $QuCN^\bullet$ can reduce O_2 with proton to produce $HO_2^\bullet$. The hydrogen abstraction of OH-adduct radical with $HO_2^\bullet$ yields phenol and H_2O_2 (Scheme 2).[56] The selectivity of formation of phenol was 98% based on the consumption of benzene after 1 h irradiation. The quantum yield was 16% at the initial stage of the photochemical reaction. After 5 h photoirradiation, the yield of phenol reached to 51%.[56] In the case of chlorobenzene with $QuCN^+$, selective formation of the corresponding phenol was also observed to afford *p*-chlorophenol and *o*-chlorophenol as 88 and 11% yield, respectively.[56]

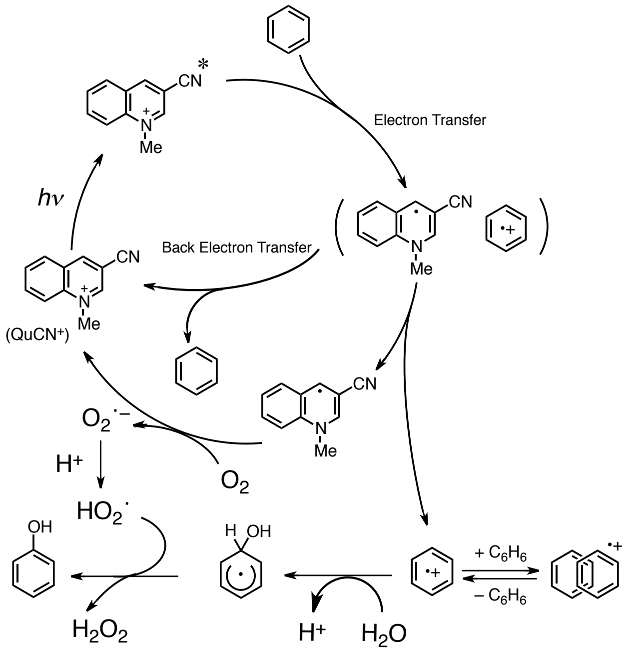

Scheme 2 Photocatalytic cycle of selective oxidation of benzene to phenol with O_2 and H_2O using $QuCN^+$ as an organic photocatalyst.

Benzene can also be oxidized using TiO_2 as a photocatalyst. In contrast to organic photocatalysts (vide supra), however, the produced phenol was overoxidized.[57] When the photocatalytic hydroxylation of benzene to phenol was conducted using TiO_2 with a phenolphilic adsorbent derived from a layered silicate under visible light irradiation, however, phenol was recovered in a high yield and purity.[57] The coexisting adsorbent that can promptly and selectively adsorb phenol from a mixture of water, benzene, and phenol separated the photocatalytically formed phenol from TiO_2 to prevent the overoxidation to diphenol, hydroquinone and *p*-benzoquinone.[57] The selective photocatalytic oxidation of benzene with O_2 and H_2O to phenol with organic photocatalysts in Scheme 1 and 2 is certainly superior to that with inorganic photocatalysts.

Selective photocatalytic alkoxylation of benzene

The selective photocatalytic oxidation of benzene with O_2 and H_2O with $QuCN^+$ to phenol has been expanded to photocatalytic alkoxylation of benezene.[58] Alkoxybenzenes are used as an important precursor to pharmaceuticals, insect pheromones and perfumes.[59] Photocatalytic alkoxylation of benzene occurred under photoirradiation of an oxygen-saturated MeCN solution containing $QuCN^+$, benzene and methanol (MeOH) with a xenon lamp (500 W, $\lambda > 290$ nm) to yield methoxybenzene and H_2O_2.[58] The yield of methoxybenzene after 4h photoirradiation was 26%.[58] When methanol was replaced by ethanol, *iso*-propanol and *tert*-butanol, the photocatalytic alkoxylation of benzene also occurred to yield the corresponding alkoxybenzenes.[58] Benzene radical cation, formed by the photoinduced electron transfer from benzene to the singlet excited state of $QuCN^+$ ($^1QuCN^{+*}$), reacts with alcohol to yield the alkoxide-adduct radical (Scheme 3).[58] The radical $QuCN^\bullet$, formed by electron transfer from benzene to $^1QuCN^{+*}$, can reduce O_2 with proton to produce $HO_2^\bullet$. The hydrogen abstraction of $HO_2^\bullet$ from OR-adduct radical affords alkoxybenzene and H_2O_2 (Scheme 3).[58]

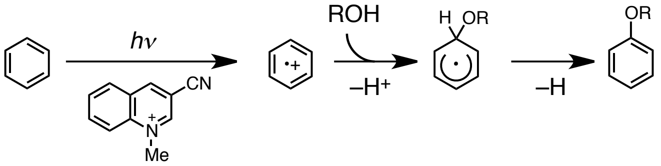

Scheme 3 Photocatalytic mechanism of selective alkoxylation via electron-transfer oxidation of benzene by $QuCN^+$ alcohol (ROH).

Intramolecular cyclization of 3-phenyl-1-propanol to chroman is known to occur via the nucleophilic capture of organic radical cations by tethered OH functions.[60,61] Thus, photocatalytic cyclization of 3-phenyl-1-propanol occurred under photoirradiation of QuCN$^+$ClO$_4^-$ in an O_2-saturated MeCN to give a cyclization product, chroman.[56] The yield of chroman was 30% after 15 min photoirradiation.[59] The photocyclization is also initiated by photoinduced electron transfer from 3-phenyl-1-propanol to ^{1}QuCN^{+*} to produce the radical cation of 3-phenyl-1-propanol (Scheme 4).[56] The cationic charge is localized on the aromatic moiety, to which the OH group attacks to yield chroman by the hydrogen abstraction with $HO_2^•$.

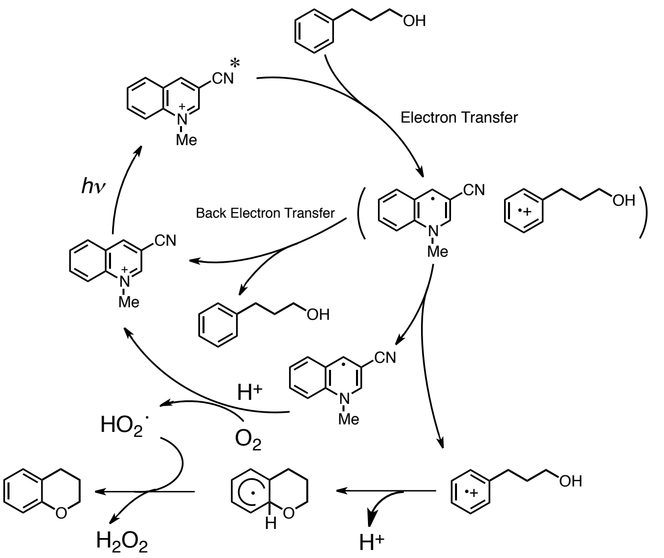

Scheme 4 Photocatalytic cycle of photocyclization of 3-phenyl-1-propanol with O_2 using QuCN$^+$ as an organic photoredox catalyst.

Selective photocatalytic monofluorination of benzene with fluoride and oxygen

Fluorination reactions of aromatic compounds have merited special attention because of useful application in the fields of material science, chemical industry and medicine.[62,63] However, it has been difficult to perform selective mono-fluorination of aromatic compounds by normal synthetic procedures.[64] Conventional fluorination reactions that afford aryl fluorides, like the Balz-Schiemann reaction where anilines are converted into aryl fluorides and the Halex process where halogen atoms are exchanged for fluorine atoms, generally require harsh conditions and consequently have limited substrate scopes.[65] An organic photocatalyst can provide a new way for fluorination of benzene with fluoride.[66] Photocatalytic fluorination of benzene occurs under photoirradiation of an oxygen-saturated MeCN solution of QuCN$^+$ containing benzene and tetraethylammonium fluoride tetrahydrofluoride (TEAF•4HF) with a xenon lamp attached with a UV-light cutting-off filter (500 W; $\lambda > 290$ nm) to yield fluorobenzene and hydrogen peroxide.[67] The yield of fluorobenzene after 50 min photoirradiation was 20% with 40% conversion of benzene.[67] Phenol was also detected as a side product because photocatalytic oxygenation of benzene with QuCN$^+$ in the presence of small amount of H_2O containing MeCN (vide supra). When benzene was replaced by fluorobenzene as a substrate, no fluorination occurred to yield difluorobenzene.[67]

The photocatalytic mechanism for monofluorination of benzene is shown in Scheme 5.[67] Benzene radical cation, produced by photoinduced electron transfer from benzene to ^{1}QuCN*, reacts with fluoride of TEAF•4HF to yield the F-adduct radical. On the other hand, the radical QuCN$^•$ reduces O_2 with proton to produce $HO_2^•$. The hydrogen abstraction of $HO_2^•$ from F-adduct radical yields fluorobenzene and H_2O_2.

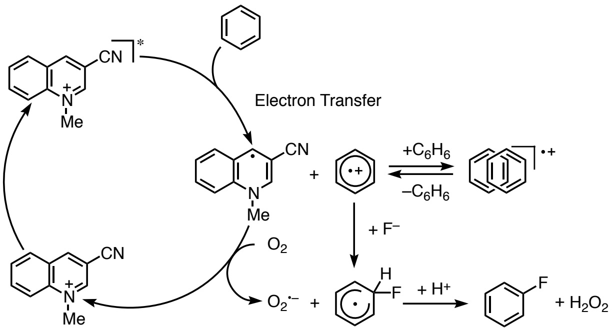

Scheme 5 Photocatalytic mechanism of monofluorination of benzene with fluoride and oxygen using QuCN$^+$ as an organic photoredox catalyst.

9-Mesityl-10-methylacridinium ion as photoredox catalyst

As described above, the excited states of organic dyes act as strong electron acceptors, which can oxidize substrates by photoinduced electron transfer. However, the photoinduced electron-transfer reactions always compete with the decay of the excited states to the ground states. The lifetimes of singlet excited states are the order of nanoseconds and those of triplet excited states are the order of microseconds. In the case of electron donor-acceptor dyad molecules (D–A), the photoexcitation affords the charge-separated states (D$^{•+}$–A$^{•-}$). The lifetimes of the charge-separated states become longer with increasing the driving force of charge recombination in the Marcus inverted region when the energy of the triplet excited state is higher than that of the charge-separated state.[16] It has been reported that 9-mesityl-10-methylacridinium ion (Acr$^+$–Mes) affords the long-lived electron-transfer (ET) state (Acr$^•$–Mes$^{•+}$), which has high oxidizing ability (E_{red} = 1.88 V *versus* SCE) and reducing ability (E_{ox} = –0.49 V *versus* SCE) in benzonitirle.[68] The X-ray crystal structure of Acr$^+$–Mes is shown in Fig. 1.[68]

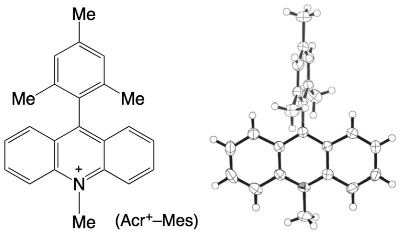

Fig. 1 Structure and ORTEP drawing of Acr$^+$–Mes.

The dihedral angle made by two aromatic ring planes is approximately perpendicular, indicating that there is no π conjugation between the donor and acceptor moieties. The ET state of Acr$^+$–Mes in solution decays via intermolecular back electron transfer in fluid solution, because the intramolecular back electron transfer is too slow.[68] Such a long lifetime of the ET state was questioned in the case of 9-(1-naphthyl)-10-methylacridinium ion (Acr$^+$–NA), because the absorption band at 700 nm due to NA$^{\bullet+}$ was not observed and the observed transient absorption spectrum in the microsecond time region was assigned to the triplet excited state.[69-71] However, the reported phosphorescence of Acr$^+$–Mes with the triplet energy of 1.96 eV[70,71] was shown to result from the acridine impurity, because Acr$^+$–Mes, which is now commercially available and synthesized according to the method without involvement of acridine, exhibits no phosphorescence.[72] The ET state (Acr$^{\bullet}$–NA$^{\bullet+}$) initially formed upon femtosecond laser excitation of Acr$^+$–NA was demonstrated to be converted to the π-dimer radical cation [(Acr$^{\bullet}$–NA$^{\bullet+}$)(Acr$^+$–NA)] via an intermolecular reaction with Acr$^+$–NA in the microsecond time region, which exhibited a broad NIR absorption at 1000 nm due to the π–π^* transition of the dimer radical cation.[73,74] The long lifetime of the ET state of Acr$^+$–Mes has allowed to observe the structural change in the Acr$^+$–Mes(ClO$_4^-$) crystal upon photoinduced ET directly by using laser pump and X-ray probe crystallographic analysis, in which the sp^2 carbon of the *N*-methyl group of Acr$^+$ is changed to the sp^3 carbon in the ET state (Acr$^{\bullet}$).[75] Furthermore, Acr$^+$–Mes has been demonstrated to act as an efficient photoredox catalyst in various organic synthetic transformations because of the high oxidizing and reducing ability of the long-lived ET state (vide infra).

Photocatalytic cycloaddition of dioxygen

The high oxidizing and reducing ability of the ET state of Acr$^+$–Mes (vide supra) provides an efficient way to produce radical cations of electron donors (D$^{\bullet+}$) and radical anions of electron acceptor (A$^{\bullet-}$) at the same time. If the direct coupling between D$^{\bullet+}$ and A$^{\bullet-}$ occurs in competition with back electron transfer from A$^{\bullet-}$ to D$^{\bullet+}$, Acr$^+$–Mes can act as an organic photoredox catalyst for the coupling between D and A. The best example of this strategy was reported for photocatalytic [2+2] cycloaddition of dioxygen (O$_2$) to tetraphenylethylene (TPE) via the electron-transfer reactions of TPE and oxygen with the ET state Acr$^+$–Mes (Scheme 6).[76] The one-electron oxidation potential of TPE (E_{ox} = 1.56 V *versus* SCE) is less positive than the value of one-electron reduction potential of Mes$^{\bullet+}$ (E_{red} = 1.88 V *versus* SCE).[76] Thus, electron-transfer oxidation of TPE with the Mes$^{\bullet+}$ moiety of Acr$^{\bullet}$–Mes$^{\bullet+}$ is thermodynamically favourable, resulting in formation of TPE$^{\bullet+}$ and Acr$^{\bullet}$–Mes. The [2+2] cycloaddition of TPE$^{\bullet+}$ with O$_2^{\bullet-}$, produced by the electron-transfer oxidation and reduction with Acr$^{\bullet}$–Mes$^{\bullet+}$, occurs efficiently in competition with back electron transfer from O$_2^{\bullet-}$ to TPE$^{\bullet+}$ to produce the 1,2-dioxetane selectively. The further photocatalytic cleavage of the O–O bond of dioxetane affords benzophenone as the final oxygenated product under photoirradiation for 90 min.[76] The second-order rate constant (k_{et}) of electron transfer from TPE to the Mes$^{\bullet+}$ moiety of Acr$^{\bullet}$–Mes$^{\bullet+}$ in Scheme 6 was determined to be 2.5 × 10^9 M^{-1} s^{-1} in CHCl$_3$ by laser flash photolysis measurements. This value is close to be the diffusion-limited value as expected from the exergonic electron transfer.[77] On the other hand, the electron- transfer reduction of O$_2$ with the Acr$^{\bullet}$ moiety of Acr$^{\bullet}$–Mes$^{\bullet+}$ also efficiently occurs, where second-order rate constant of electron transfer (k'_{et}) is 3.8 × 10^8 M^{-1} s^{-1}. The 1,2-dioxetane was isolated by column chromatography. The isolated yield was 27% after 4h photoirradiation.[76] The quantum yield of 1,2-dioxetane increases with an increase in concentration of TPE to approach a limiting value as 0.17 and 0.022 in CHCl$_3$ and MeCN, respectively.[77]

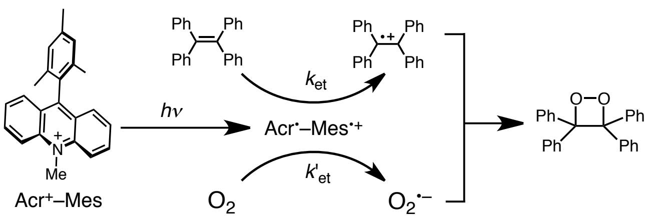

Scheme 6 Photocatalytic [2+2] cycloaddition of O$_2$ to tetraphenylethylene (TPE) via photoinduced electron transfer.

In general, the most common preparation of 1,2-dioxetanes is through the formal [2+2] cycloaddition of singlet oxygen (^{1}O$_2$) to electron-rich alkenes.[78] If alkenes are too electron poor to react with ^{1}O$_2$, however, no oxygenated products were obtained. For example, it was reported that no products were formed in an oxygen-saturated MeCN solution of TPE in the presence of ^{1}O$_2$ sensitizers such as [60]fullerene and porphyrin derivative under photoirradiation.[79] Thus, the photocatalytic cycloaddition of O$_2$ to alkenes with Acr$^+$–Mes provides a unique pathway to synthesize dioxetanes of electron poor alkenes.[76]

Acr$^+$–Mes also acts as an efficient photoredox catalyst for the *cis-trans* isomerization of stilbene via the radical cation (Scheme 7).[80] It is known that *cis-trans* isomerization occurs rapidly in the stilbene radical cation.[77] The steady-state *cis-trans* ratio of stilbene has been reported to be 98.8 : 1.[77] The observed yield of *trans*-stilbene from *cis*-stilbene was 96% after

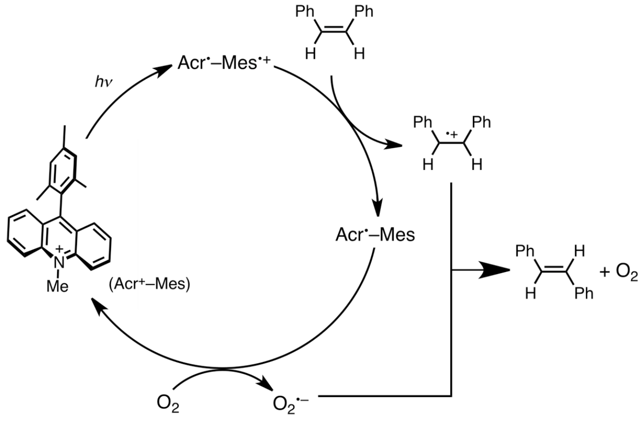

Scheme 7 Photocatalytic *cis-trans* isomerization of stilbene with Acr$^+$–Mes.

60 min photoirradiation, when the total consumption of *cis*- and *trans*-stilbene by the photocatalytic oxidation by O_2 was still 4%.[77]

When anthracene derivatives are used as substrates, Acr^+–Mes acts as an efficient photoredox catalyst for [4+2] cycloaddition of O_2 to anthracene derivatives to afford the corresponding epidioxyanthracenes via the radical coupling between the radical cations of anthracene derivatives and $O_2^{\bullet-}$, which are produced by the electron-transfer oxidation and reduction of anthracene derivatives and O_2 by the ET state of Acr^+–Mes, respectively (Scheme 8).[81] In the case of 9,10-dimethylanthracene (DMA), the yield of dimethylepidioxyanthracene was 99% and no further oxidation occurred.[81] In the case of anthracene, however, the further photoirradiation results in formation of anthraquinone as the final six-electron oxidation product via 10-hydroxyanthrone, accompanied by formation of H_2O_2.[81]

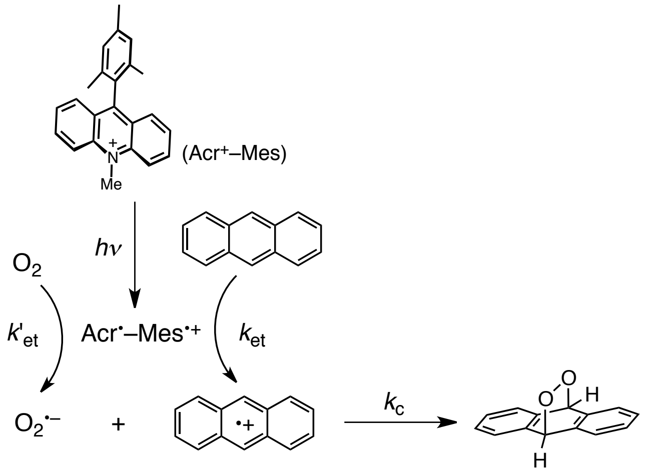

Scheme 8 Photocatalytic [4+2] cycloaddition of O_2 to anthracene.

The second-order rate constant (k_{et}) of electron transfer from DMA to the $Mes^{\bullet+}$ moiety of $Acr^{\bullet}$–$Mes^{\bullet+}$ was determined to be 1.4×10^{10} M^{-1} s^{-1} in MeCN at 298 K, which is close to be the diffusion-limited value as expected from the exergonic electron transfer.[82] The rate constant of electron transfer from the $Acr^{\bullet}$ moiety of $Acr^{\bullet}$–$Mes^{\bullet+}$ to O_2 (k'_{et}) was also determined to be 6.8×10^8 M^{-1} s^{-1} in MeCN at 298 K. The [4+2] cycloaddition of O_2 to anthracene is known to occur also by the reaction of anthracene with singlet oxygen ($^1O_2$).[82,83] In order to evaluate the contribution of the singlet oxygen pathway, the rate constant of the reaction of $^1O_2$ with DMA was determined by emission decay rates of $^1O_2$ (λ_{em} = 1270 nm)[84,85] in the presence of various concentrations of DMA to be 2.4×10^5 M^{-1} s^{-1}.[81] This value is much smaller than the second-order rate constant (k_c) of the radical coupling between $DMA^{\bullet+}$ and $O_2^{\bullet-}$ (1.7×10^{10} M^{-1} s^{-1}).[81] It was confirmed that no singlet oxygen emission was observed during the photocatalytic oxygenation of DMA with Acr^+–Mes in an O_2-saturated CD_3CN.[81] Thus, the [4+2] cycloaddition of O_2 to anthracene occurs exclusively by the radical coupling between anthracene radical cation and $O_2^{\bullet-}$ rather than the reaction of anthracene and $^1O_2$, although the both pathways yield the same product.

Selective photocatalytic oxygenation of *p*-xylene

Photocatalytic oxygenation of *p*-xylene with O_2 also occurs under visible light irradiation of $[Acr^+–Mes]ClO_4^-$ (λ_{max} = 430 nm) in oxygen-saturated MeCN containing *p*-xylene (4.0 mM) to yield the oxygenated product, *p*-tolualdehyde (34%), *p*-methylbenzyl alcohol (10%) and the reduced product of O_2, H_2O_2 (30%).[81] The photocatalytic reactivity was enhanced by the presence of H_2O (0.9 M) and sulphuric acid (1.0 mM) to yield *p*-tolualdehyde (75%), *p*-methylbenzyl alcohol (15%) and H_2O_2 (74%) with a high quantum yield (0.25).[86] The 100% yield of *p*-tolualdehyde and H_2O_2 with a higher quantum yield (0.37) was achieved by using 9-mesityl-2,7,10-trimethylacridinium ion (Me_2Acr^+–Mes), where the hydrogens at 2 and 7 positions of the acridinium ring are replaced by the methyl groups.[86] The E_{red} value of Me_2Acr^+–Mes (–0.67 V *versus* SCE) is by 0.1 eV more negative than that of Acr^+–Mes (–0.57 V), indicating that the $Me_2Acr^{\bullet}$ moiety acts as a stronger electron donor. The rate constants of the electron-transfer reduction of O_2 were determined from the quenching of the transient absorption due to the ET state by O_2 to be 6.8×10^8 M^{-1} s^{-1} for $Acr^{\bullet}$–$Mes^{\bullet+}$ and 2.0×10^{10} M^{-1} s^{-1} for $Me_2Acr^{\bullet}$–$Mes^{\bullet+}$ in MeCN at 298 K.[86] Thus, the reducing ability of $Me_2Acr^{\bullet}$–$Mes^{\bullet+}$ was significantly enhanced by the electron-donating methyl substitution of the acridinium ring of Acr^+–Mes. This may be the reason why the 100% yield of tolualdehyde and H_2O_2 with a higher quantum yield (0.37) was achieved by using Me_2Acr^+–Mes (vide infra). No further oxygenated product, *p*-toluic acid or *p*-phthaladehyde, was produced during the photocatalytic reaction.

The photocatalytic oxygenation also occurred using durene and mesitylene as substrates.[83] The E_{ox} values of toluene derivatives are lower than the one-electron reduction potential (E_{red}) of the ET state of R_2Acr^+–Mes ($R_2Acr^{\bullet}$–$Mes^{\bullet+}$; R = H and Me: 2.06 V *versus* SCE in MeCN).[86] Thus, electron transfer from toluene derivatives such as *p*-xylene to the $Mes^{\bullet+}$ moiety of $R_2Acr^{\bullet}$–$Mes^{\bullet+}$ is energetically feasible, whereas electron transfer from toluene (E_{ox} = 2.20 V)[51] to the $Mes^{\bullet+}$ moiety is energetically unfavourable when no photocatalytic oxidation of toluene by O_2 occurred with Acr^+–Mes under the same experimental conditions.[86] The E_{ox} values of the oxygenated products of the corresponding benzaldehydes are also higher than the E_{red} value of $R_2Acr^{\bullet}$–$Mes^{\bullet+}$.[86] This is the reason why the selective oxygenaton of *p*-xylene to *p*-tolualdehyde was achieved without further oxygenation of *p*-tolualdehyde.

The photocatalytic reaction is also initiated by electron transfer from *p*-xylene to the $Mes^{\bullet+}$ moiety of $R_2Acr^{\bullet}$–$Mes^{\bullet+}$ to produce *p*-xylene radical cation, which undergoes fast deprotonation to afford the deprotonated radical. This is followed by rapid O_2 addition to afford the peroxyl radical. The disproportionation of the peroxyl radical affords *p*-tolualdehyde, *p*-methylbenzyl alcohol and O_2. *p*-Methylbenzyl alcohol is readily oxygenated to yield *p*-tolualdehyde with $Acr^{\bullet}$–$Mes^{\bullet+}$.[86] On the other hand, $O_2^{\bullet-}$ undergoes the disproportionation with proton to yield H_2O_2 and O_2 (Scheme 9). The radical intermediates involved in Scheme 9 were detected by EPR ($g_{//}$ = 2.101, $g_{\perp}$ = 2.009 for $O_2^{\bullet-}$ and $g_{//}$ = 2.033, $g_{\perp}$ = 2.006 for *p*-methylbenzylperoxyl radical) in frozen MeCN).[86]

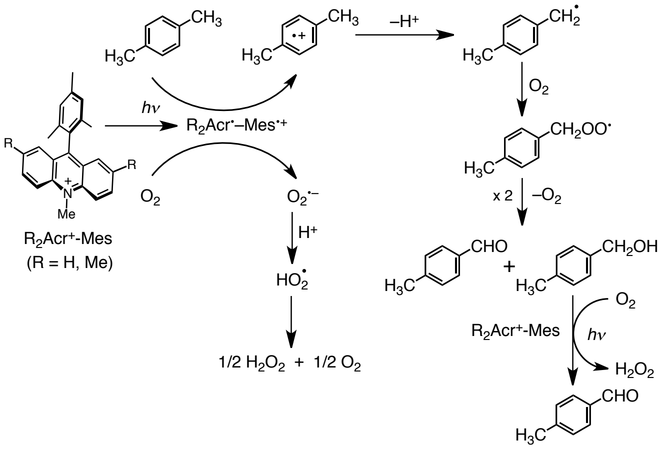

Scheme 9 Reaction scheme of photocatalytic oxygenation of *p*-xylene and formation of H_2O_2 catalyzed by R_2Acr^+–Mes.

Addition of aqueous sulphuric acid enhanced the deprotonation of *p*-xylene radical cation and the disproportionation process of $O_2^{\bullet-}$, respectively, leading to a remarkable enhancement of photocatalytic reactivity as mentioned above.[86] The photocatalytic reactivity and stability of Acr^+–Mes was further improved by incorporating Acr^+-Mes into mesoporous silica-alumina with an copper complex $[(tmpa)Cu^{II}]^{2+}$ (tmpa = tris(2-pyridylmethyl)amine) for the selective oxygenation of *p*-xylene by O_2 to produce *p*-tolualdehyde,[87] because the $[(tmpa)Cu^{II}]^{2+}$ complex acts as an efficient catalyst for the O_2 reduction.[88,89]

Methyl-substituted naphthalenes were also oxygenized with O_2 using Acr^+–Mes as a photoredox catalyst.[90,91] It should be noted that 2-methylnaphthalene does not react with $^1O_2$ to produce no oxygenated products.[90] This underscores the utility of Acr^+–Mes in photocatalytic oxygenation of substrates as compared with $^1O_2$ photosensitizers. Photocatalytic oxidation of triphenylphosphine (Ph_3P) and benzylamine ($PhCH_2NH_2$) with O_2 also occurs efficiently using Acr^+–Mes as an photoredox catalyst to yield $Ph_3P{=}O$ and $PhCH_2N{=}CHPh$, respectively.[92]

Photocatalytic oxidative bromination of aromatic hydrocarbons with hydrogen bromide and oxygen

Bromination of aromatic compounds has been one of the most important and fundamental reactions in organic synthesis, providing key precursors for various transformations such as Grignard reactions and Suzuki-Miyaura coupling.[93] Electrophilic bromination in nature mainly occurs by oxidative bromination through the catalyzed oxidation of the halide ion to form a brominating reagent, whereas bromination is usually carried out with hazardous, toxic, and corrosive molecular bromine, which is better to be avoided from the ecological point of view.[94] The best candidate for oxidants would be oxygen since hydrogen peroxide or water would be the only side product.[94] In this context, Acr^+–Mes was reported to act as an efficient organic photocatalyst for the oxidative bromination of aromatic hydrocarbons by O_2 with hydrogen bromide to produce the monobrominated products selectively.[95] Both the product yield and selectivity for the bromination of 1,3,5-trimethoxybenzene (TMB) were 100% with a quantum yield of 4.8%.[95] The photocatalytic turnover number was 900 based on the initial concentration of Acr^+–Mes.[95] When methoxy-substituted aromatic compounds were replaced by toluene derivatives, the consumption of substrate occurred efficiently under the same experimental conditions.[95] However, the yield of the brominated product and selectivity were significantly lower as compared with methoxy-substituted benzenes, because the photobromination competes with photooxygenation with oxygen to yield the corresponding aromatic aldehyde (Scheme 9).[95]

The photocatalytic reaction is also initiated by intramolecular photoinduced electron transfer from the Mes moiety to the singlet excited state of the Acr^+ moiety of Acr^+–Mes to generate the ET state ($Acr^\bullet$–$Mes^{\bullet+}$) as shown in Scheme 10, where the $Mes^{\bullet+}$ moiety can oxidize TMB to produce $TMB^{\bullet+}$, whereas the $Acr^\bullet$ moiety can reduce O_2 with proton to $HO_2^\bullet$.[95] The $TMB^{\bullet+}$ reacts with Br^- to form the Br–adduct radical, which undergoes dehydrogenation with $HO_2^\bullet$ to afford the corresponding monobrominated product and hydrogen peroxide. Hydrogen peroxide further reacts with HBr and the substrate to produce another monobrominated product and H_2O.[95] The selectivity of mono-bromination resulted from the lower reactivity of the radical cations of brominated benzenes with Br^-.[95] Although the substrates that can be brominated are limited by their one-electron oxidation potentials, which should be less positive than the E_{ox} value of Acr^+–Mes (2.06 V *versus* SCE), this limitation is compensated for by the high selectivity for the bromination to avoid over-bromination.[95] When HBr was replaced by HCl, photocatalytic chlorination of aromatic substrates with Acr^+–Mes also occurred under otherwise the same experimental conditions.[96]

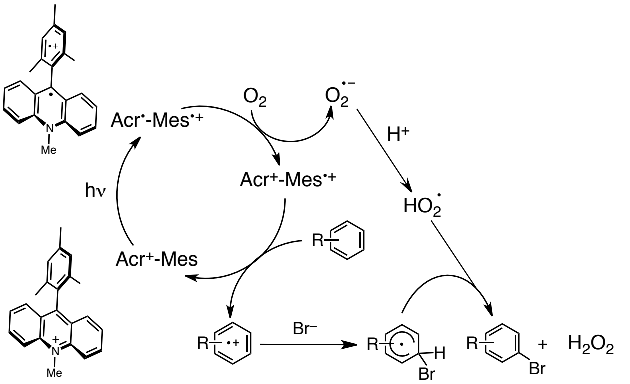

Scheme 10 Photocatalytic mechanism of bromination of aromatic compounds with HBr and O_2 using Acr^+–Mes as an organic photocatalyst.

Photocatalytic intramolecular anti-Markovnikov hydroetherification of alkenols

Nicewicz and a coworker recently utilized the high oxidizing ability of the ET state of Acr^+–Mes for the anti-Markovnikov hydroetherification of alkenols with 2-phenylmalononitrile as a redox-cycling source of a H-atom, with complete regioselectivity without any trace of the undesired Markovnikov regioisomer.[97,98] The utility of Acr^+–Mes as a organic photoredox catalyst is underscored when compared directly with the frequently employed $[\mathrm{Ru(bpy)_3}]^{2+}$, which failed to give any of the desired product.[97] The high oxidizing ability of the ET state of $\mathrm{Acr^+}$–Mes allowed for greater latitude in potential substrates with alkenes possessing the one-electron oxidation potentials ranging up to +2.0 V *versus* SCE.[97]

The photocatalytic cycle is shown in Scheme 11.[97] The ET state of $\mathrm{Acr^+}$–Mes oxidizes the alkenol via the electron transfer from the alkenol to the $\mathrm{Mes^{\bullet+}}$ moiety of the ET state to produce the corresponding radical cation, which is cyclised followed by H-atom transfer from 2-phenylmalononitrile. the resulting radical could serve as an oxidant for the $\mathrm{Acr^\bullet}$ radical to produce the carbanion, regenerating the ground state $\mathrm{Acr^+}$–Mes. Proton transfer from the cyclised cation to the carbanion regenerates the H-atom donor (2-phenylmalononitrile) and yields the desired product (Scheme 11).[97] The scope of the intramolecular anti-Markovnikov hydroalkoxylation of alkenols was examined ranging from electron-rich (4-(MeO)$\mathrm{C_6H_4}$, 80% yield) to electron-deficient (4-Cl$\mathrm{C_6H_4}$, 60% yield) compounds provided good yields of the desired 5-exo adducts.[97] The anti-Marcovnikov hydroetherification of alkenols shows sharp contrast to Brønsted acid assisted Markovnikov hydroetherification.[97]

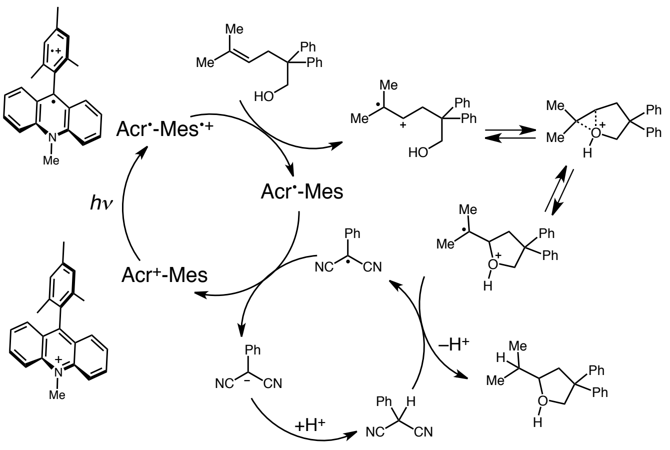

Scheme 11 Photocatalytic cycle for intramolecular anti-Markovnikov hydroetherification of alkenols.

The same strategy used for intramolecular hydroetherification of alkenols where the radical cations gave rise to anti-Markovnikov reactivity in Scheme 11 has also been applied for intramolecular anti-Markovnikov hydroamination of unsaturated amines in which thiophenol was used as a hydrogen-atom donor.[99] The photocatalytic system is effective for a range of cyclization modes to give important nitrogen-containing heterocycles.[99]

Photocatalytic cycloaddition between alkenes with alkenols

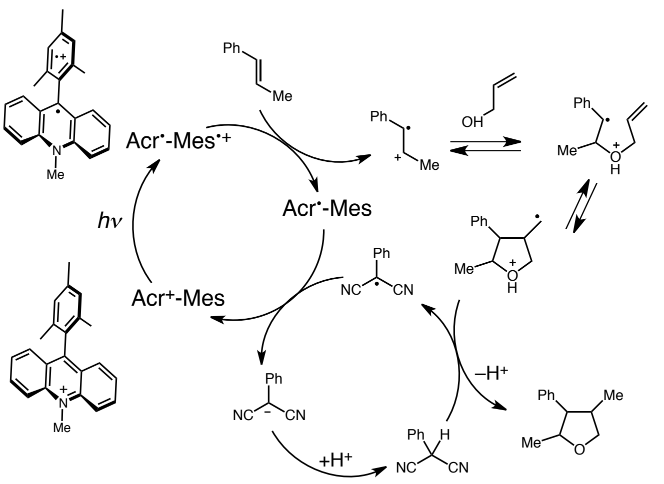

Scheme 12 Photocatalytic cycle of intermolecular cycloaddition between β-methylstyrene and allyl alcohol.

The intramolecular anti-Markovnikov hydroetherification of alkenols in Scheme 11 has been extended to intermolecular cycloaddition of *trans*-β-methylstyrene and allyl alcohol in Scheme 12.[100] The β-methylstyrene radical cation produced by electron transfer from β-methylstyrene to the ET state of $\mathrm{Acr^+}$–Mes reacts with allyl alcohol to produce the adduct radical cation, which undergoes a 5-exo radical cyclization with the pendant alkene.[100] Hydrogen-atom abstraction from 2-phenylmalononitrile and the loss of a proton yields the tetrahydrofuran adduct (63% yield).[100] The phenyl malononitrile anion is neutralized by the generated proton to regenerate the hydrogen-atom donor (2-phenylmalonitrile).[100] Employing *cis*-β-methylstyrene gave an identical mixture of diastereomers as *trans*-β-methylstyrene (80 % yield), demonstrating the loss of alkene geometry upon the one-electron oxidation.[100] 4-Chloro-β-methylstyrene gave the corresponding tetrahydrofuran adduct in good yield (70% yield), whereas 4-methoxy-β-methylstyrene was not reactive under these conditions, probably due to the stability of the resultant radical cation intermediate.[100] Cyclic alkene substrates, such as indene and 1-phenylcyclohexene also afforded good yields of the corresponding cyclic ether adducts.[95] Aliphatic trisubstituted alkenes with higher oxidation potentials, such as 2-methylbut-2-ene, also afforded highly substituted cyclic ethers.[100] Thus, $\mathrm{Acr^+}$–Mes is used as an effective organic photoredox catalyst to synthesize highly substituted tetrahydrofurans from readily available allylic alcohols and alkenes.[100]

Photocatalytic intermolecular anti-Markovnikov addition of carboxylic acids to alkenes

The photocatalytic cycle in intermolecular cycloaddition between β-methylstyrene and allyl alcohol in Scheme 12 has also been applied to anti-Markovnikov hydroacetoxylation of styrenes, trisubstituted aliphatic alkenes and enamides, with a variety of carboxylic acids to afford the anti-Markovnikov addition adducts exclusively (Scheme 13).[101] Electron-transfer oxidation of the alkene by the $\mathrm{Mes^{\bullet+}}$ moiety of the ET state of $\mathrm{Acr^+}$–Mes results in formation of the alkene cation radical to

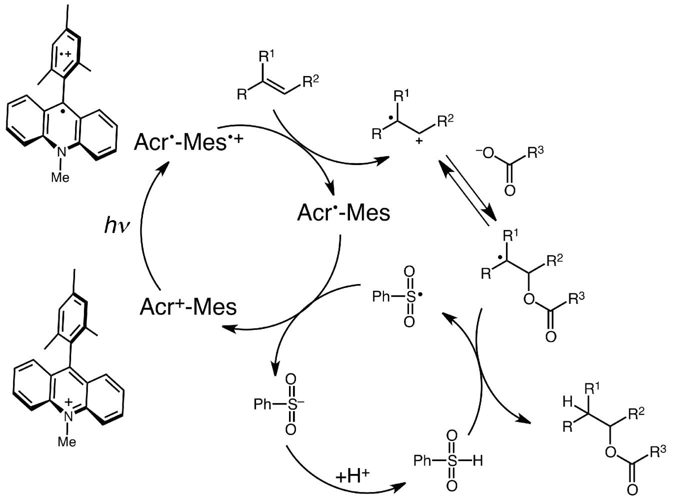

Scheme 13 Photocatalytic cycle of anti-Markovnikov alkene hydroacetoxylation.

which the carboxylate nucleophile is added to the less substituted position of the cation radical to produce the adduct radical.[101] A rapid acid-base equilibrium with the excess carboxylic acid generates small quantities of benzenesulfinic acid, which acts as the active hydrogen-atom donor.[101] Hydrogen-atom transfer from benzenesulfinic acid to yield the anticipated anti-Markovnikov adduct.[101] The hydrogen-atom transfer step is found to be the rate-determining because of large deuterium kinetic isotope effect.[101] The resultant benzenesulfinyl radical oxidizes the $\text{Acr}^\bullet$ moiety to regenerate Acr^+–Mes and benzenesulfinate.[101]

Photocatalytic hydrotrifluoromethylation of styrenes and unactivated aliphatic alkenes

The development of new methodologies for highly efficient and selective incorporation of a CF_3 group into diverse skeletons has merited significant interest of synthetic chemists,[102] because the CF_3 group is a useful structural motif in many biologically active molecules as well as materials.[102] There have been several reports on photocatalytic trifluoromethylation using metal complexes as photosensitizers.[104-107] Nicewicz and a coworker recently reported metal-free hydrotrifluoromethylation of alkenes using Acr^+–Mes as an efficient organic photoredox catalyst as shown in Scheme 14.[108]

The electron-transfer oxidation of sodium trifluoromethanesulfinate (CF_3SO_2Na, Langlois reagent)[109] results in formation of the electrophilic trifluroromethyl radical ($CF_3^\bullet$) together with expulsion of SO_2. Addition of $CF_3^\bullet$ to the alkene occurs with anti-Markovnikov selectivity to produce the corresponding carbon-centred radical.[108] Alkyl-substituted alkenes provided hydrotrifluoromethylated products without the use of thiols as an H-atom donor.[108] In this case, trifluoroethanol used as a cosolvent acts as an H-atom donor. The produced trifluoromethylketyl radical oxidizes the $\text{Acr}^\bullet$ moiety of $\text{Acr}^\bullet$-Mes to regenerate Acr^+–Mes. Methyl thiosalicylate is used as an H-atom donor for aliphatic alkenes, and thiophenol is used as an H-atom donor for styrenyl substrates.[108] The substrate scope for the photocatalytic trifluoromethylation is broad, including mono-, di- and trisubstituted aliphatic and styrenyl alkenes, with high regioselectivity.[108]

Photocatalytic C-C bond formation

Acr^+–Mes can also be used as an effective photoredox catalyst for C-C bond formation of deprotonated radicals following formation of the radical cations of substrates (vide infra). Although photoexcitation of anthracene gives a [4+4] dimer through the singlet excimer intermediate,[110,111] another type of anthracene dimer derivative, i.e., dimethyllepidopterene (5,6,11,12-tetrahydro-4b,12[1',2'],6,10b[1",2"]-dibenzenochrysene) has been prepared by photocatalytic carbon-carbon bond formation of 9,10-dimethylanthracene (DMA) in chloroform via the electron-transfer oxidation of DMA with the ET state of Acr^+–Mes (Scheme 15).[112] Visible light irradiation ($\lambda > 430$ nm) of the absorption band of Acr^+–Mes (5.0×10^{-4} M) in a deaerated chloroform ($CDCl_3$) solution containing DMA (1.5×10^{-3} M) results in formation of dimethyllepidopterene, 1,2-bis(9-anthracenyl)ethane, and 9-(β,β-dichloroethyl)-10-methylanthracene (Scheme 15).[112] The isolated yield of dimethyllepidopterene was 12% after 4h photoirradiation at 298 K.[112] The ORTEP drawing determined from the X-ray crystal structural analysis is also shown in Scheme 15.[112] The bond length of the newly formed C-C bond (C6-C6') is 1.629(2) Å, which is much longer than normal C-C single bonds due to the severe distortion of this compound.[112]

The electron transfer from DMA to the $\text{Mes}^\bullet$ moiety of $\text{Acr}^\bullet$–$\text{Mes}^{\bullet+}$ is followed by deprotonation from the methyl group of $\text{DMA}^{\bullet+}$ and the radical coupling reaction between 9-

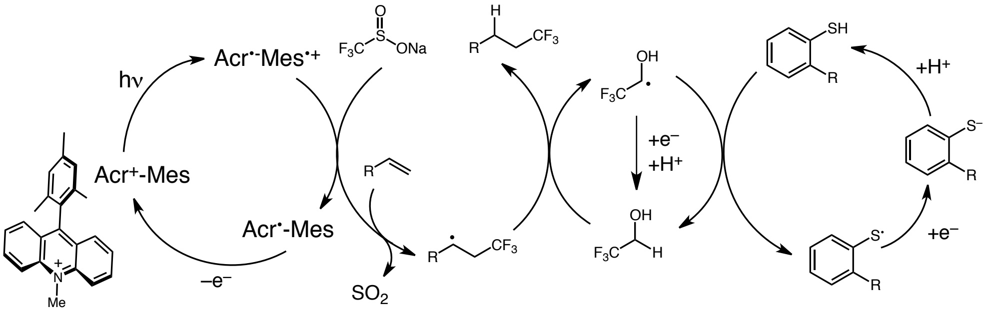

Scheme 14 Photocatalytic cycle of trifluoromethylation of alkenes.

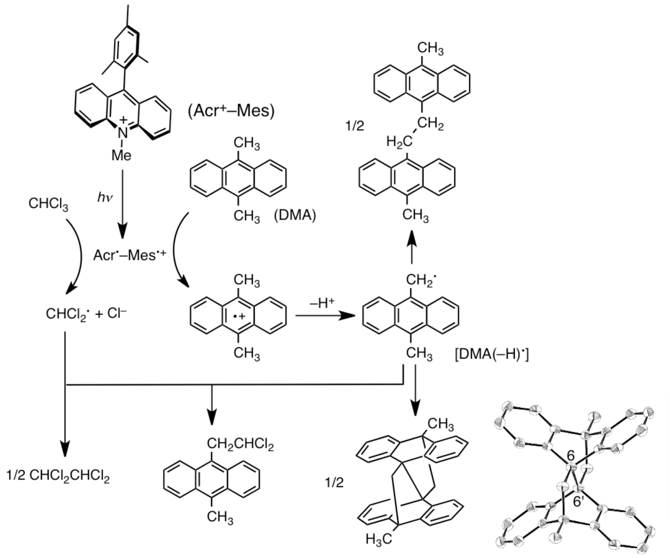

Scheme 15 Photocatalytic cycle of dimerization of 9,10-diemthylanthracene and the ORTEP drawing of lepidopterene determined by X-ray crystal structural analysis.

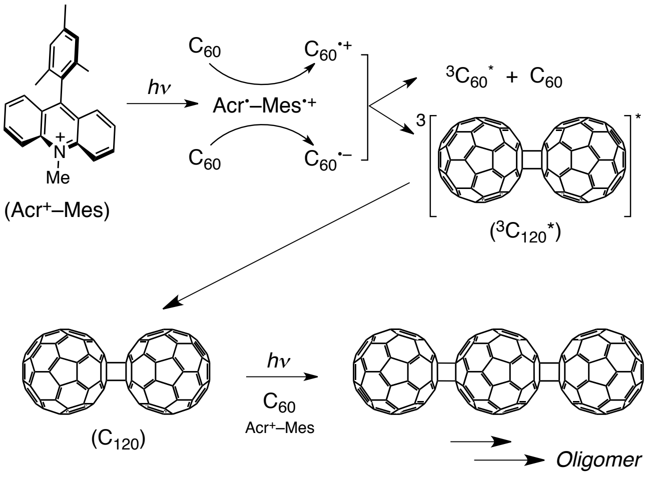

Scheme 16 Photocatalytic cycle of oligomerization of C_{60} with Acr^{+}–Mes.

methylanthrylmethyl radicals occurs to yield dimethyllepidopterene together with 1,2-bis(9-anthracenyl)ethane.[112] The $Acr^{\bullet}$–Mes, produced by electron transfer from DMA to $Acr^{\bullet}$–$Mes^{\bullet+}$, was oxidized by dissociative electron transfer to $CHCl_3$ to produce $CHCl_2^{\bullet}$ and Cl^{-}. The $CHCl_2^{\bullet}$ radicals dimerized to yield 1,1,2,2-tetrachloroethane ($CHCl_2CHCl_2$) or reacted with 9-methylanthrylmethyl radical to yield 9-(β,β-dichloroethyl)-10- methyl- anthracene (Scheme 15).[112] The deprotonation from the methyl group of $DMA^{\bullet+}$ is the key step for formation of dimethyllepidopterene. Thus, no photodimerization has occurred in the case of unsubstituted anthracene, which has no methyl group to be deprotonated, or 9,10-diethylanthracene in which the deprotonation from the ethyl group may be too slow to complete with the back electron transfer.[112] The acceleration of the deprotonation of $DMA^{\bullet+}$ by the presence a base such as tetra-*n*-butylammonium hydroxide (TBAOH) resulted in improvement of the isolated yield of dimethyllepidopterene (21%) as compared with the yield in the absence of a base (12%).[112]

The C-C bond formation also occurs between the radical cation and radical anion of the same substrate, which are formed by the electron-transfer oxidation and reduction of the substrate by $Acr^{\bullet}$–$Mes^{\bullet+}$. For example, photocatalytic oligomerization of fullerene in toluene/acetonitrile solution occurs efficiently via the electron-transfer oxidation and reduction of C_{60} with $Acr^{\bullet}$–$Mes^{\bullet+}$, followed by the radical coupling reaction between $C_{60}^{\bullet+}$ and $C_{60}^{\bullet-}$ (Scheme 16).[113] Because the free energy change of electron transfer (ΔG_{et}) from C_{60} (E_{ox} = 1.73 V *versus* SCE)[114] to the $Mes^{\bullet+}$ moiety of $Acr^{\bullet}$–$Mes^{\bullet+}$ (E_{red} = 1.88 V) in benzonitrile (PhCN) is negative (ΔG_{et} = –0.15 eV), the electron-transfer oxidation C_{60} is energetically feasible to form $C_{60}^{\bullet+}$. On the other hand, the electron-transfer reduction of C_{60} (E_{red} = –0.43 V) with the $Acr^{\bullet}$ moiety of $Acr^{\bullet}$–$Mes^{\bullet+}$ (E_{ox} = –0.49 V) is also thermodynamically feasible to give $C_{60}^{\bullet-}$ (ΔG_{et} = –0.06 eV).[113] Thus, C_{60} acts as both an electron donor and acceptor in the electron-transfer reactions of $Acr^{\bullet}$–$Mes^{\bullet+}$ with C_{60} to produce $C_{60}^{\bullet+}$ and $C_{60}^{\bullet-}$ together at the same time. The [2+2]cycloaddition occurs efficiently between $C_{60}^{\bullet+}$ and $C_{60}^{\bullet-}$ to afford the triplet excited state ($^3C_{120}^{*}$), because the driving force of charge recombination (2.16 eV) is larger than the triplet excited state energy of C_{120} (ca. 1.5 eV).[115] Further oligomerization occurs by the same process.[113]

Photocatalytic cycloreversion of photochromic dithienylethene compounds

Photocatalytic cycloreversion (ring opening) of photochromic *cis*-1,2-dithienylethene (DTE) compounds[116] occurs efficiently using Acr^{+}–Mes as a photoredox catalyst.[117] Thus, not only C-C bond formation (vide supra) but also C-C bond cleavage of the closed form of DTE has been achieved using the photoredox catalysis of Acr^{+}–Mes.[117] An exergonic electron transfer from DTE to the $Mes^{\bullet+}$ moiety of $Acr^{\bullet}$–$Mes^{\bullet+}$ initiates the ring opening of DTE (initiation) in competition with the back ET from the $Acr^{\bullet}$ moiety to the radical cation of the closed form (Scheme 17). The electron transfer from a closed form of neutral DTE to the open form radical cation completes cycloreversion to regenerate the closed form radical cation. This is the propagation step of the electrocatalytic chain mechanism in Scheme 17. The chain process is terminated by

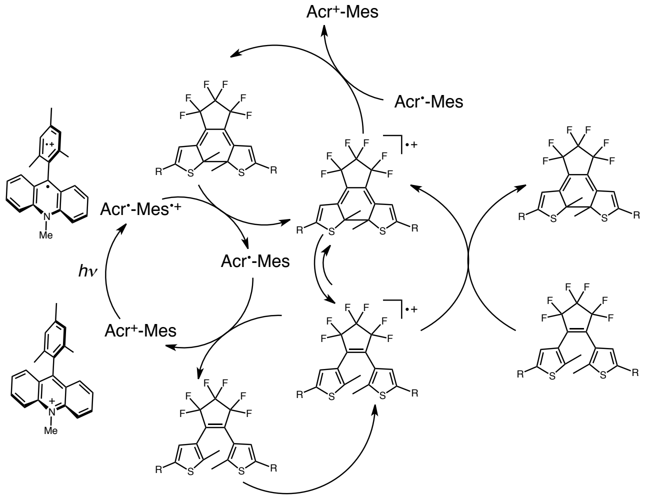

Scheme 17 Photoinduced electron-transfer chain mechanism of the photoelectrocatalytic cycloreversion of DTE compounds with $\mathrm{Acr^+}$–Mes. R = pyridyl, phenyl, 4-methoxyphenyl and 3,4-dimethoxyphenyl.

back electron transfer from $\mathrm{Acr^\bullet}$–Mes to the open form radical cation (termination).[117] This strategy benefits from the catalytic nature of the electrochromism; in contrast to the photon-stoichiometric photochromism, the photon economy gains a leverage effect, leading to greatly improved the quantum yield.[117]

Conclusions

A variety of novel organic synthetic transformations have been made possible by organic photoredox catalysis via photoinduced electron-transfer reactions. In particular, the use of the excited states of 2,3-dichloro-5,6-dicyano-*p*-benzoquinone (DDQ) and 3-cyano-1-methylquinolinium ion ($\mathrm{QuCN^+}$), which have strong oxidizing ability has made it possible to oxygenate benzene to phenol via formation of benzene radical cation. An electron donor-acceptor linked dyad, 9-mesityl-10-methylacridinium ion ($\mathrm{Acr^+}$–Mes) can be used as an efficient photoredox catalyst, because the long-lived electron-transfer state of $\mathrm{Acr^+}$–Mes, produced upon photoexcitation, can oxidize and reduce external electron donors and acceptors to produce the corresponding radical cations and radical anions, respectively, leading to selective oxygenation, halogenation, C–C bond formation and cleavage of various substrates. Thus, metal free photocatalytic reactions via photoinduced electron transfer of organic photosensitizers and donor-acceptor dyads provide new ways to achieve environmentally benign organic synthesis. Photocatalytic organic synthesis can be finely controlled by choosing appropriate organic photocatalysts with tuned one-electron redox potentials. The scope and the applications of organic photoredox catalytic systems are expected to expand much further in the future.

Acknowledgements

The authors gratefully acknowledge the contributions of their collaborators and coworkers mentioned in the cited references, and support by an ALCA fund from Japan Science and Technology Agency (JST) and funds from the Ministry of Education, Culture, Sports, Science and Technology (MEXT), Japan.

Notes and references

1 N. S. Lewis and D. G. Nocera, *Proc. Natl. Acad. Sci. U .S. A.*, 2006, **103**, 15729-15735.
2 T. A. Faunce, W. Lubitz, A. W. Rutherford, D. MacFarlane, G. F. Moore, P. Yang, D. G. Nocera, T. A. Moore, D. H. Gregory, S. Fukuzumi, K. B. Yoon, F. A. Armstrong and M. R. Wasielewski, *Energy Environ. Sci*., 2013, **6**, 695-698.
3 H. B. Gray, *Nature Chem*., 2009, **1**, 7.
4 M. D. Kärkäs, E. V. Johnston, O. Verho and B. Åkermark, *Acc. Chem. Res*., 2014, **47**, 100-111.
5 S. Fukuzumi and Y. Yamada, *ChemSusChem*, 2013, **6**, 1834-1847.
6 J. J. Concepcion, R. L. House, J. M. Papanikolas and T. J. Meyer, *Proc. Nat. Acad. Sci. U. S. A.,* 2012, **109**, 15560-15564.
7 S. Fukuzumi, D. Hong and Y. Yamada, *J. Phys. Chem. Lett*., 2013, **4**, 3458-3467.
8 V. Balzani, A. Credi and M. Venturi, *ChemSusChem*, 2008, **1**, 26-58.
9 S. Fukuzumi, *Eur. J. Inorg. Chem.,* 2008, *9*, 1351-1362.
10 S. Fukuzumi, Y. Yamada, T. Suenobu, K. Ohkubo and H. Kotani, *Energy Environ. Sci*., 2011, **4**, 2754-2766.
11 D. Gust, T. A. Moore and A. L. Moore, *Acc. Chem. Res*., 2009, **42**, 1890-1898.
12 G. Bottari, G. de la Torre, D. M. Guldi and T. Torres, *Chem. Rev*., 2010, **110**, 6768-6816.
13 S. Fukuzumi and K. Ohkubo, *J. Mater. Chem*., 2012, **22**, 4575-4587.
14 M. R. Wasielewski, *Acc. Chem. Res*., 2009, **42**, 1910-1921.
15 S. Fukuzumi, K. Ohkubo and T. Suenobu, *Acc. Chem. Res*., 2014, **79**, 1455-1464.
16 S. Fukuzumi, *Phys. Chem. Chem. Phys*., 2008, **10**, 2283-2297.
17 F. D'Souza and O. Ito, *Chem. Commun*., 2009, 4913-4928.
18 S. Fukuzumi and T. Kojima, *J. Mater. Chem*., 2008, **18**, 1427-1439.
19 F. D'Souza and O. Ito, *Chem. Soc. Rev*., 2012, **41**, 86-96.
20 S. Fukuzumi, K. Ohkubo, F. D'Souza and J. L. Sessler, *Chem. Commun*., 2012, **48**, 9801-9815.
21 K. Ohkubo and S. Fukuzumi, *Bull. Chem. Soc. Jpn*., 2009, **82**, 303-315.
22 K. Ohkubo and S. Fukuzumi, *J. Porphyrins Phthalocyanines,* 2008, **12**, 993-1004.
23 S. Fukuzumi and K. Ohkubo, In *Encyclopedia of Radicals in Chemistry, Biology and Materials*, ed. C. Chatgilialoglu and A. Studer, John Wiley & Sons, Ltd., Chichester, UK, 2012, vol. 1, pp. 365-393.
24 M. A. Ischay and T. P. Yoon, *Eur. J. Org. Chem*., 2012, 3359-3372.
25 M. Fagnoni, D. Dondi, D. Ravelli and A. Albini, *Chem. Rev*., 2007, **107**, 2725-2756.
26 X. Lang, X. Chen and J. Zhao, *Chem. Soc. Rev*., 2014, **43**, 473-486.
27 H. Kisch, *Angew. Chem., Int. Ed*., 2013, **52**, 812-847.
28 I. Paramasivam, H. Jha, N. Liu and P. Schmuki, *Small*, 2012, **8**, 3073-3103.
29 G. Palmisano, E. Garcia-Lopez, G. Marci, V. Loddo, S. Yurdakal, V. Augugliaro and L. Palmisano, *Chem. Commun*., 2010, **46**, 7074-7089.
30 M. A. Lazar and W. A. Daoud, *RSC Adv*., 2013, **4**, 4130-4140.
31 G. Palmisano, V. Augugliaro, M. Pagliaro and L. Palmisano, *Chem. Commun*., 2007, 3425-3437.
32 D. Ravelli, M. Fagnoni and A. Albini, *Chem. Soc. Rev*., 2013, **42**, 97-113.
33 S. Fukuzumi and K. Ohkubo, *Chem. Sci*., 2013, **4**, 561-574.
34 C. K. Prier, D. A. Rankic and D. W. C. MacMillan, *Chem. Rev*., 2013, **113**, 5322-5363.

35 L. Shi and W. Xia, *Chem. Soc. Rev.*, 2012, **41**, 7687-7697.

36 J. W. Tucker and C. R. J. Stephenson, *J. Org. Chem.*, 2012, **77**, 1617-1622.

37 J. M. R. Narayanam and C. R. J. Stephenson, *Chem. Soc. Rev.*, 2011, **40**, 102-113.

38 T. Koike and M. Akita, *Synlett*, 2013, **24**, 2492-2505.

39 M. Weber, M. Weber and M. Kleine-Boymann, *Phenol. Ullmann's Encyclopedia of Industrial Chemistry*, Wiley-VCH, Weinheim, 2004.

40 R. J. Schmidt, *Appl. Catal. A*, 2005, **280**, 89-103.

41 S. Niwa, M. Eswaramoorthy, J. Nair, A. Raj, N. Itoh, H. Shoji, T. Namba and F. Mizukami, *Science*, 2002, **295**, 105-107.

42 Z. Long, Y. Zhou, G. Chen, P. Zhao and J. Wang, *Chem. Eng. J.*, 2014, **239**, 19-25.

43 W. Wang, G. Ding, T. Jiang, P. Zhang, T. Wu and B. Han, *Green Chem.*, 2013, **15**, 1150-1154.

44 C. Zhou, J. Wang, Y. Leng and H. Ge, *Catal. Lett.*, 2010, **135**, 120-125.

45 Y. Liu, K. Murata and M. Inaba, *J. Mol. Catal. A: Chem.*, 2006, **256**, 247-255.

46 R. Bal, M. Tada, T. Sasaki and Y. Iwasawa, *Angew. Chem., Int. Ed.*, 2006, ***45***, 448-452.

47 L. Wang, S. Yamamoto, S. Malwadkar, S. Nagamatsu, T. Sasaki, K. Hayashizaki, M. Tada and Y. Iwasawa, *ChemCatChem*, 2013, **5**, 2203-2206.

48 K. Ohkubo, A. Fujimoto and S. Fukuzumi, *J. Am. Chem. Soc.*, 2013, **135**, 5368-5371.

49 Z. Shen, J. Dai, J. Xiong, X. He, W. Mo, B. Hu, N. Sun and X. Hu, *Adv. Synth. Catal.*, 2011, **353**, 3031-3038.

50 P. B. Merkel, P. Luo, J. P. Dinnocenzo and S. Farid, *J. Org. Chem.*, 2009, **74**, 5163-5173.

51 S. Fukuzumi, K. Ohkubo, T. Suenobu, K. Kato, M. Fujitsuka and O. Ito, *J. Am. Chem. Soc.*, 2001, **123**, 8459-8467.

52 S. M. Hubig, T. M. Bockman and J. K. Kochi, *J. Am. Chem. Soc.*, 1997, **119**, 2926.

53 B. Badger and B. Brocklehurst, *Nature*, 1968, **219**, 263-263.

54 K. Okamoto, S. Seki and S. Tagawa, *J. Phys. Chem. A*, 2006, *110*, 8073-8080.

55 R. A. Marcus, *Angew. Chem., Int. Ed. Engl.*, 1993, **32**, 1111-1121.

56 K. Ohkubo, T. Kobayashi and S. Fukuzumi, *Angew. Chem., Int. Ed.*, 2011, **50**, 8652-8655.

57 Y. Ide, M. Torii and T. Sano, *J. Am. Chem. Soc.*, 2013, **135**, 11784-11786.

58 K. Ohkubo, T. Kobayashi and S. Fukuzumi, *Opt. Exp.*, 2012, **20**, A360-A365.

59 H. Fiege, H.-W. Voges, T. Hamamoto, S. Umemura, T. Iwata, H. Miki, Y. Fujita, H.-J. Buysch, D.; Garbe and W. Paulus, *Phenol Derivatives in Ullmann's Encyclopedia of Industrial Chemistry*, Wiley-VCH, Weinheim, 2002.

60 H. Togo and M. Katohgi, *Synlett*, 2001, 565-581.

61 S. Furuyama and M. Katohgi, *Synlett*, 2010, 2325-2329.

62 K. Müller, C. Faeh and F. Diederich, *Science*, 2007, **317**, 1881-1886.

63 H. Amii and K. Ueyama, *Chem. Rev.*, 2009, **109**, 2119-2183.

64 M. Shimizu and T. Hiyama, *Angew. Chem., Int. Ed.*, 2005, **44**, 214-231.

65 T. Furuya, S. Adam, A. S. Kamlet and T. Ritter, *Nature*, 2011, **473**, 470-477.

66 H. H. Meurs, D. W. Sopher and W. Eisenberg, *Angew. Chem., Int. Ed. Engl.*, 1989, **28**, 927‑928.

67 K. Ohkubo, A. Fujimoto and S. Fukuzumi, *J. Phys. Chem. A*, 2013, **117**, 10719-10725.

68 S. Fukuzumi, H. Kotani, K. Ohkubo, S. Ogo, N. V. Tkachenko and H. Lemmetyinen, *J. Am. Chem. Soc.*, 2004, **126**, 1600-1601.

69 J. W. Verhoeven, H. J. van Ramesdonk, H. Zhang, M. M. Groeneveld, A. C. Benniston and A. Harriman, *Int. J. Photoenergy*, 2005, **7**, 103-108.

70 A. C. Benniston, A. Harriman, P. Li, J. P. Rostron and J. W. Verhoeven, *Chem. Commun.*, 2005, 2701-2703.

71 A. C. Benniston, A. Harriman, P. Li, J. P. Rostron, H. J. van Ramesdonk, M. M. Groeneveld, H. Zhang and J. W. Verhoeven, *J. Am. Chem. Soc.*, 2005, **127**, 16054–16064.

72 K. Ohkubo, H. Kotani and S. Fukuzumi, *Chem. Commun.*, 2005, 4520-4522.

73 S. Fukuzumi, H. Kotani and K. Ohkubo, *Phys. Chem. Chem. Phys.*, 2008, **10**, 5159-5162.

74 H. Kotani, K. Ohkubo and S. Fukuzumi, *Faraday Discuss.*, 2012, **155**, 89-102.

75 M. Hoshino, H. Uekusa, A. Tomita, S. Koshihara, T. Sato, S. Nozawa, S. Adachi, K. Ohkubo, H. Kotani and S. Fukuzumi, *J. Am. Chem. Soc.*, 2012, **134**, 4569-4572.

76 K. Ohkubo, T. Nanjo and S. Fukuzumi, *Org. Lett.*, 2005, **7**, 4265-4268.

77 K. Ohkubo, T. Nanjo and S. Fukuzumi, *Catal. Today*, 2006, **117**, 356-361.

78 T. Wilson and A. P. Schaap, *J. Am. Chem. Soc.*, 1971, **93**, 4126-4136.

79 P. A. Burns and C. S. Foote, *J. Am. Chem. Soc.*, 1974, **96**, 4339-4340.

80 F. D. Lewis, A. M. Bedell, R. E. Dykstra, J. E. Elbert, I. R. Gould and S. Farid, *J. Am. Chem. Soc.*, 1990, **112**, 8055-8064.

81 H. Kotani, K. Ohkubo and S. Fukuzumi, *J. Am. Chem. Soc.*, 2004, **126**, 15999-16006.

82 C. S. Foote, *Acc. Chem. Res.*, 1968, **1**, 104-110.

83 J.-M. Aubry, C. Pierlot, J. Rigaudy and R. Schmidt, *Acc. Chem. Res.*, 2003, **36**, 668-675.

84 S. Fukuzumi, S. Fujita, T. Suenobu, H. Yamada, H. Imahori, Y. Araki and O. Ito, *J. Phys. Chem. A*, 2002, **106**, 1241-1247.

85 S. Fukuzumi, K. Ohkubo, X. Zheng, Y. Chen, R. K. Pandey, R. Zhan and K. M. Kadish, *J. Phys. Chem. B*, 2008, **112**, 2738-2746.

86 K. Ohkubo, K. Mizushima, R. Iwata, K. Souma, N. Suzuki and S. Fukuzumi, *Chem. Commun.*, 2010, ***46***, 601-603.

87 S. Fukuzumi, K. Doi, A. Itoh, T. Suenobu, K. Ohkubo, Y. Yamada and K. D Karlin,. *Proc. Natl. Acad. Sci. U. S. A.*, 2012, **109**, 15572-15577.

88 S. Fukuzumi, H. Kotani, H. R. Lucas, K. Doi, T. Suenobu, R. Peterson and K. D. Karlin, *J. Am. Chem. Soc.*, 2010, **132**, 6874-6875.

89 S. Kakuda, R. L. Peterson, K. Ohkubo, K. D. Karlin and S. Fukuzumi, *J. Am. Chem. Soc.*, 2013, **135**, 6513-6522.

90 A. G. Griesbeck and M. Cho, *Org. Lett.*, 2007, **9**, 611-613.

91 H. Kotani, K. Ohkubo and S. Fukuzumi, *Appl. Catal. B Environ.*, 2008, **77**, 317-324.

92 K. Ohkubo, T. Nanjo and S. Fukuzumi, *Bull. Chem. Soc. Jpn.*, 2006, **79**, 1489-1500.

93 V. V. K. M. Kandepi and N. Narender, *Synthesis*, 2012, **44**, 15-26.

94 A. Podgorsek, M. Zupan and J. Iskra, *Angew. Chem., Int. Ed.*, 2009, **48**, 8424-8450.

95 K. Ohkubo, K. Mizushima, R. Iwata and S. Fukuzumi, *Chem. Sci.*, 2011, **2**, 715-722.

96 K. Ohkubo, K. Mizushima and S. Fukuzumi, *Chem. Res. Intermed.*, 2013, **39**, 205-220.

97 D. S. Hamilton and D. A. Nicewicz, *J. Am. Chem. Soc.*, 2012, **134**, 18577-18580.

98 D. A. Nicewicz and T. M. Nguyen, *ACS Catal.*, 2014, **4**, 355-360.

99 T. M. Nguyen and D. A. Nicewicz, *J. Am. Chem. Soc.*, 2013, **135**, 9588-9591.

100 J.-M. M. Grandjean and D. A. Nicewicz, *Angew. Chem., Int. Ed.*, 2013, **52**, 3967-3971.

101 A. J. Perkowski and D. A. Nicewicz, *J. Am. Chem. Soc.*, 2013, **135**, 10334-10337.

102 T. Furuya, A. S. Kamlet, T. Ritter, *Nature*, 2011, **473**, 470-477.

103 K. Müller, C. Faeh and F. Diederich, *Science*, 2007, **317**, 1881-1886.

104 D. A. Nagib, M. E. Scott and D. W. C. MacMillan, *J. Am. Chem. Soc.*, 2009, **131**, 10875-10877.

105 N. Iqbal, J. Jung, S. Park and E. J. Cho, *Angew. Chem., Int. Ed.*, 2014, **53**, 539-542.

106 Y. Yasu, T. Koike and M. Akita, *Chem. Commun.*, 2013, **49**, 2037-2039.

107 Y. Yasu, T. Koike and M. Akita, *Angew. Chem., Int. Ed.*, 2012, **51**, 9567-9571.

108 D. J. Wilger, N. J. Gesmundo and D. A. Nicewicz, *Chem. Sci.*, 2013, **4**, 3160-3165.

109 B. R. Langlois, E. Laurent and N. Roidot, *Tetrahedron Lett.*, 1991, *32*, 7525-7528.

110 J. L. Charlton, R. Dabestani and J. Saltiel, *J. Am. Chem. Soc.*, 1983, **105**, 3473-3476.

111 S. Fukuzumi, T. Okamoto and K. Ohkubo, *J. Phys. Chem. A*, 2003, **107**, 5412-5418.

112 K. Ohkubo, R. Iwata, S. Miyazaki, T. Kojima and S. Fukuzumi, *Org. Lett.*, 2006, **8**, 6079-6082.

113 K. Ohkubo, R. Iwata, T. Yanagimoto and S. Fukuzumi, *Chem. Commun.*, 2007, 3139-3142.

114 D. Dubois, G. Moninot, W. Kutner, M. T. Jones and K. M. Kadish, *J. Phys. Chem.*, 1992, **96**, 7137-7145.

115 M. Fujitsuka, C. Luo, O. Ito, Y. Murata and K. Komatsu, *J. Phys. Chem. A*, 1999, *103*, 7155-7160.

116 M. Irie, *Chem. Rev.*, 2000, **100**, 1685-1716.

117 S. Lee, Y. You, K. Ohkubo, S. Fukuzumi and W. Nam, *Angew. Chem., Int. Ed.,* 2012, **51**, 13154-13158.

TOC

Organic Synthetic Transformations using Organic Dyes as Photoredox Catalysts

Shunichi Fukuzumi and Kei Ohkubo

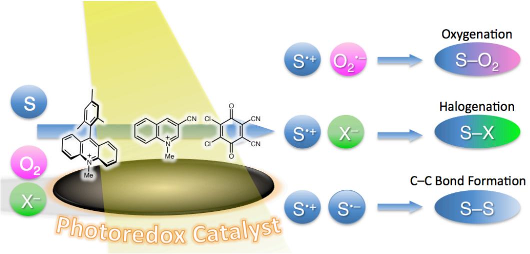

This review article presents various photocatalytic transformation such as oxygenation, halogenation and C-C bond formation with organic photoredox catalysts.